Received: 1 June 2016 | Revised: 19 August 2016 | Accepted: 12 September 2016 | Published on: 5 January 2017

DOI: 10.1002/ctpp.201600043

ORIGINAL PAPER

Contributions to Plasma Physics

Heat flow through a plasma sheath in the presence of secondary electron emission from plasma-wall interaction

Jing Ou[1,2*] | Xiaoyun Zhao[1]

[1]Institute of Plasma Physics, Chinese Academy of Sciences, Hefei, China
[2]Center for Magnetic Fusion Theory, Chinese Academy of Sciences, Hefei, China

***Correspondence**

Jing Ou, Institute of Plasma Physics, Chinese Academy of Sciences, Hefei 230031, China.
E-mail: ouj@ipp.ac.cn

Funding Information
This research was supported by the National Natural Science Foundation of China, 11475223, 11105176. National Magnetic Confinement Fusion Science Programme of China, 2015GB101003. Programme of Fusion Reactor Physics and Digital Tokamak with the CAS "One-Three-Five" Strategic Planning,

The formation of a plasma sheath in front of a negative wall emitting secondary electron is studied by a one-dimensional fluid model. The model takes into account the effect of the ion temperature. With the secondary electron emission (SEE) coefficient obtained by integrating over the Maxwellian electron velocity distribution for various materials such as Be, C, Mo, and W, it is found that the wall potential depends strongly on the ion temperature and the wall material. Before the occurrence of the space-charge-limited (SCL) emission, the wall potential decreases with increasing ion temperature. The variation of the sheath potential caused by SEE affects the sheath energy transmission and impurity sputtering yield. If SEE is below SCL emission, the energy transmission coefficient always varies with the wall materials as a result of the effect of SEE, and it increases as the ion temperature is increased. By comparison of with and without SEE, it is found that sputtering yields have pronounced differences for low ion temperatures but are almost the same for high ion temperatures.

KEYWORDS
energy transmission coefficient, plasma sheath, secondary emission electron, sputtering yield

1 | INTRODUCTION

The characteristics of a plasma sheath located between a plasma and a material surface play an important role in the plasma heat flow to the material surface during plasma–wall interaction. Several key factors influence the sheath structure, including electron emission,[1–11] magnetic field,[11–15] ion temperature,[13–15] and collision.[15–17] The most important one is the electron emission from plasma–wall interaction. It greatly reduces the sheath potential so that the thermal insulation may become substantially low because the potential drop across the sheath is a potential barrier for the incoming plasma electrons. The emission electron flux through the sheath may be regulated by the space-charge-limited (SCL) effect. The investigation of the plasma sheath in the presence of secondary electron emission (SEE) has been carried out based on several models.[1–6] However, many models consider cold ions, whereas the effect of ion temperature has not been studied systematically. For the edge plasma in fusion devices, the ion temperature is comparable to or higher than the electron temperature.[18–21] In addition, it is shown from sheath model results that the ion temperature influences the sheath properties.[13–15] Since the ion temperature in the tokamak edge region is important for the estimation of heat flux flowing to material surface and modelling plasma–wall interaction processes including impurity sputtering,[19] here we describe a plasma sheath with thermal ions in the presence of SEE.

When heat flows through the plasma sheath, the sheath energy transmission coefficient γ, defined as the energy flux normalized by the particle exhaust flux times the electron temperature at the sheath entrance,[22] is used to estimate the energy flux flowing to the target plate in fusion device experiments and to provide boundary conditions in fusion plasma edge fluid codes. γ increases when SEE is taken into account or as the ion temperature is increased for a given SEE coefficient.[23] Another important physical process affected by the sheath structure is impurity production. Intrinsic impurities (e.g., Be, C, Mo, and W) are produced through erosion during the energy load on the plasma-facing material. The impurity sputtering yield depends

strongly on the ion temperature[24] and the sheath potential.[10] Therefore, it is of great interest to investigate the sheath energy transmission and impurity sputtering yields during heat flow through a plasma sheath in the presence SEE for a wide range of ion temperatures.

2 | SHEATH MODEL

As seen in Figure 1 for a one-dimensional sheath model, an infinitely large planar wall located at $x=0$ has its surface perpendicular to the x-axis. The wall is not only the sink that all the particles impact upon but also the source of SEE. The potential profile in the sheath is determined by the following Poisson equation:

$$\frac{d^2\phi}{dx^2} = -\frac{e_0}{\varepsilon_0}(n_i - n_{e1} - n_{e2}), \tag{1}$$

where ϕ is the potential, e_0 is the elementary charge, ε_0 is the permittivity of free space, n_i is the density of the singly charged positive ions, n_{e1} is the primary electron density, and n_{e2} is the emitted electron density. We define the sheath edge at the position $x=d$, which is the last point where the quasi-neutrality is still valid. At distance from $x=d$ to the wall, the plasma quasi-neutrality breaks down and the region is the sheath region. The region located between the bulk plasma region and the potion $x=d$ is the pre-sheath region in which the potential decreases slowly but the plasma is still considered quasi-neutral. Usually, the sheath thickness d is much larger than the Debye length $\lambda_D = \sqrt{(\varepsilon_0 k_B T_e)/(n_{e10} e_0^2)}$, where n_{e10} is the primary electron density at the sheath edge, while the length scale of the pre-sheath, L, is much larger than d. In the limit $\lambda_D/L \to 0$, the electric field at the sheath edge is zero, that is,

$$\frac{d\phi}{dx}|_{x=d} = 0. \tag{2}$$

Inside the sheath, any collisions are negligible based on the assumption that the sheath is thin enough. Therefore, the ion flux and energy are conserved:

$$n_i(x)v_i(x) = n_{i0}v_{i0}, \tag{3}$$

$$\frac{1}{2}m_i v_i^2(x) + e_0\phi(x) = \frac{1}{2}m_i v_{i0}^2, \tag{4}$$

where n_{i0} and v_{i0} are the ion density and the velocity at the sheath edge, respectively, and x refers to a position in the sheath $x<d$. From Equations 3 and 4, we can obtain:

$$n_i(x) = n_{i0}\left(\frac{0.5m_i v_{i0}^2}{0.5m_i v_{i0}^2 - e_0\phi(x)}\right)^{1/2}. \tag{5}$$

The primary electron density satisfies the Boltzmann relation in our model, that is,

$$n_{e1}(x) = n_{e10}\exp\left(\frac{e_0\phi(x)}{k_B T_e}\right) \tag{6}$$

and the flux of the primary electron at the wall can be written as,

$$\Gamma_{e1} = \frac{1}{4}n_{e10}\exp\left(\frac{e_0\phi_S}{k_B T_e}\right)\sqrt{\frac{8k_B T_e}{\pi m_e}}, \tag{7}$$

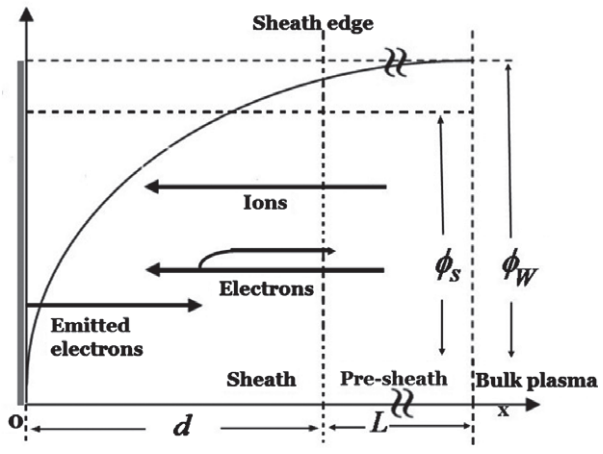

FIGURE 1 Schematic of the sheath model. The pre-sheath length L is much larger than the sheath thickness d, which is much larger than the Debye length λ_D. The potential decreases monotonically towards the wall, and the potential drop across the sheath is ϕ_S.When the emission is SCL, the electric field at the wall surface is zero.

where ϕ_S is the potential drop across the sheath.

It is assumed that the flux of the emitted electrons, Γ_{e2}, is one dimensional and perpendicular to the wall surface:

$$\Gamma_{e2} = n_{e2}(x)v_{e2}(x) \tag{8}$$

and that all the emitted electrons leave the wall with the negligible initial velocity, though their initial velocity may influence the sheath.[4,9] Then the energy of the emitted electrons in the sheath can be written as,

$$\frac{1}{2}m_e v_{e2}^2(x) - e_0\phi(x) = -e_0\phi_S. \tag{9}$$

Making use of Equations 8 and 9, we can obtain the profile of emitted electron density in the sheath as,

$$n_{e2}(x) = \frac{\Gamma_{e2}}{\sqrt{\frac{-2e_0[\phi_S-\phi(x)]}{m_e}}}. \tag{10}$$

At the sheath edge, quasi-neutrality is valid, so the ion density at the sheath edge can be expressed as,

$$n_{i0} = n_{e10} + \Gamma_{e2}/\sqrt{\frac{-2e_0\phi_S}{m_e}} \tag{11}$$

If a stable sheath where the potential is a monotonically decreasing function is formed in front of a negative wall, the ion velocity entering the sheath is equal to or larger than the ions' sound velocity C_s, that is, $v_{i0} \geq C_s$. This is the well-known Bohm criterion.[25] For a plasma containing more than one population of negatively charged particles, the Bohm criterion can be written as,[26]

$$v_{i0} \geq \sqrt{\frac{k_B(\gamma_p T_i + T_e^{scr})}{m_i}}. \tag{12}$$

Here, γ_p is the polytropic coefficient, and T_e^{scr} is the electron screening temperature, defined as $T_e^{scr} = \frac{e_0 n_e(\phi)}{k_B dn_e/d\phi}|_{\phi=0}$, where n_e can be obtained from the Equations 6 and 10. Clearly, v_{i0} will depend on ϕ_s if SEE is taken into account. In our case, the Bohm criterion is fulfilled in a marginal form, that is, with the equality sign, and $\gamma_p = 1$ for isothermal approximation is considered.

At the wall, we have the following relation due to the current balance in a floating sheath:

$$\Gamma_i = \Gamma_{e1} - \Gamma_{e2} \text{ or } \Gamma_i = (1 - \delta_{eff})\Gamma_{e1}, \tag{13}$$

where δ_{eff} is the effective electron emission coefficient. Here, the electron emission mechanism is specified as SEE. Usually, the ion-induced SEE is not important unless the ion impact energy is greater than 1 keV, while the electron-induced SEE is significant even at rather modest energies, that is, >30 eV.[27] In this paper, we only take into account the SEE due to the impact of electrons against the wall.

For simplicity, we introduce the following variables:

$$\varphi = \frac{e_0\phi}{k_B T_e},\ F_{e2} = \frac{\Gamma_{e2}}{n_{e10}\sqrt{k_B T_e/m_e}},\ \mu = \frac{m_e}{m_i},\ u_i = \frac{v_i}{\sqrt{k_B T_e/m_i}},\ T_{eff} = \frac{T_i + T_e^{scr}}{T_e},\ z = \frac{x}{\lambda_D},\ \alpha = \frac{T_i}{T_e}. \tag{14}$$

The normalized Poisson's equation, expressed purely in terms of the potential, is obtained by combining Equations 5, 6, and 10 with Equation 11:

$$\frac{d^2\varphi}{dz^2} = \exp(\varphi) + F_{e2}/\sqrt{-2(\varphi_S - \varphi)} - \sqrt{\frac{T_{eff}}{T_{eff} - 2\varphi}}[1 + F_{e2}/\sqrt{-2\varphi_S}]. \tag{15}$$

By multiplying $d\varphi/dz$ on both sides of Equation 15 and then integrating from the sheath edge to z, we get the following equation:

$$\begin{aligned}\frac{1}{2}\left(\frac{d\varphi}{dz}\right)^2 &= \exp(\varphi) - 1 + F_{e2}[\sqrt{-2(\varphi_S - \varphi)} - \sqrt{-2\varphi_S}] \\ &\quad + [\sqrt{T_{eff}(T_{eff} - 2\varphi)} - T_{eff}][1 + F_{e2}/\sqrt{-2\varphi_S}],\end{aligned} \tag{16}$$

where $d\varphi/dz$ is the dimensionless electric field. When SEE is present, for the case in which the sheath potential is monotonic, the electron field at the wall satisfies:

$$\exp(\varphi_S) - 1 - F_{e2}\sqrt{-2\varphi_S} + T_{eff}(\sqrt{1 - 2\varphi_S/T_{eff}} - 1)(1 + F_{e2}/\sqrt{-2\varphi_S}) \geq 0. \tag{17}$$

Inequality (17) is valid when the electron emission is below the SCL region. If the electron field at the wall is zero, the electron emission is SCL.

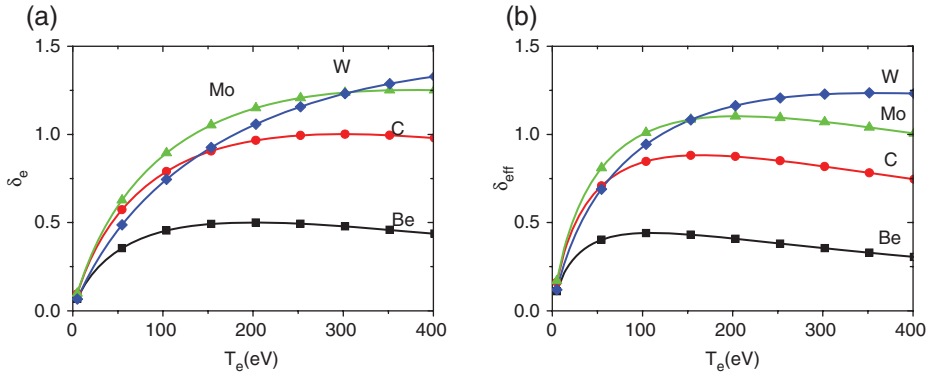

FIGURE 2 (a) SEE coefficient obtained from the Sternglass formula, and (b) effective SEE coefficient obtained from Equation 19 for the Maxwellian distribution electrons.

On the other hand, the normalized Equation 13 can be expressed as,

$$\frac{1}{\sqrt{2\pi}}\exp(\varphi_S) - F_{e2} = \sqrt{\mu T_{eff}}\left(1 + F_{es}/\sqrt{-2\varphi_S}\right) = (1-\delta_{eff})\frac{1}{\sqrt{2\pi}}\exp(\varphi_S). \tag{18}$$

If the electrons obey a non-Maxwellian electron energy distribution, δ_{eff} depends on both the sheath potential and their energy when they impinge the material surface.[7]. However, for a Maxwellian distribution of the electrons, it does not depend on sheath potential, but is usually a function of the electron temperature.[2,7,28] By using the Sternglass formula $\delta_e(\varepsilon) = \delta_m \frac{\varepsilon}{\varepsilon_m}\exp(2 - 2\sqrt{\varepsilon/\varepsilon_m})$,[29] where $\delta_{\rm m}$ is the maximum of δ_e, and $\varepsilon_{\rm m}$ is the characteristic energy corresponding to $\sigma_{\rm m}$, δ_{eff} can be expressed as,[28]

$$\delta_{eff}(T_e) = (2.72)^2\frac{\delta_m}{k_B T_e}\int_0^\infty \frac{E_p}{E_{pm}}\exp\left[-\frac{E_p}{k_B T_e} - 2\left(\frac{E_p}{E_{pm}}\right)^{1/2}\right]dE_p. \tag{19}$$

As seen in Equation 19, if the temperature of the Maxwellian-distributed electrons impinging the wall is known, φ_w and v_{i0} can be obtained by solving Equations 12 and 18 for a given value of α. During this calculation, the inequality in (17) is checked. If the solutions of φ_w and v_{i0} correspond to a stable sheath whose SEE is below SCL, the inequality in (17) will be satisfied. If the solution is marginal, the equality in (17) is met, indicating that SEE is SCL. It must be pointed out that our analysis finds a stable sheath solution corresponding to SCL for which the electric field at the wall vanishes. Using the current method, we cannot address whether there exists a stable sheath with non-vanishing electric field at the wall.

Because the large SEE may cause a very large influx of the emission electrons, SCL may be broken and then a virtual cathode can be formed in front of the wall.[1,11,30] To ensure that (17) is valid, we discuss δ_e and δ_{eff} for materials that are used widely in tokamak, such as beryllium (Be, $\delta_{\rm m} = 0.5$, $E_{\rm pm} = 200$ eV), carbon (C, $\delta_{\rm m} = 1.0$, $E_{\rm pm} = 300$ eV), molybdenum (Mo, $\delta_{\rm m} = 1.25$, $E_{\rm pm} = 375$ eV), and tungsten (W, $\delta_{\rm m} = 1.4$, $E_{\rm pm} = 650$ eV). Figure 2 shows the SEE coefficients obtained from Sternglass formula and the effective SEE obtained by integrating over the Maxwellian electron velocity distribution for the four materials. For low temperatures ($T_e < 50$ eV), δ_{eff} is larger than δ_e, and the secondary electron coefficient is significantly smaller than unity. For high temperatures (100 eV $< T_e <$ 400 eV), δ_{eff} is smaller than δ_e, and secondary electron coefficients for Mo and W are larger than unity. According to the results obtained by Hobbs and Wesson,[1] $\delta_{eff} \sim 0.82$ for a stable cold ion sheath when the electron emission is SCL. As seen in Figure 2b, the sheath may be in the SCL state for C, Mo, or W as wall materials. In the following discussion, we will focus on the effects of SEE on the plasma sheath when SEE is below the SCL state.

3 | NUMERICAL RESULTS

In this section, we show some results of the model described in the previous section for a hydrogen plasma with 2 eV $< T_e <$ 40 eV. Since α in a tokamak depends strongly on macroscopic parameters such as the plasma density or heating power, there is no "typical" value of α in the edge region.[20] Here we choose $0 \le \alpha \le 5$ to investigate the effect of the ion temperature on the sheath properties based on the facts that the ion temperature is comparable to or higher than the electron temperature in several tokamaks[18–21] and that the sheath with cold ions ($T_i = 0$) has been studied by several sheath models.[1,2] After we discuss the sheath potential, we present the sheath energy transmission coefficient and impurity sputtering yields for various materials such as Be, C, Mo, and W.

First, we analyse the dependence of the sheath potential on the wall material. Figure 3a shows the profiles of the normalized sheath potential as a function of electron temperature for the four different materials in the case of $\alpha = 1.0$. We can see that the normalized sheath potential decreases with increase in the electron temperature. This is due to the fact that δ_{eff} and the resulting

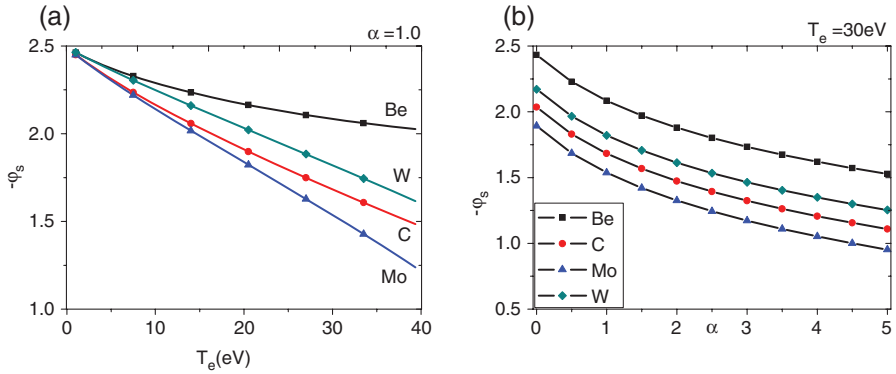

FIGURE 3 Normalized sheath potential for Be, C, Mo, and W walls as a function of (a) electron temperature with $\alpha = 1.0$ and (b) α with $T_e = 30\,\text{eV}$.

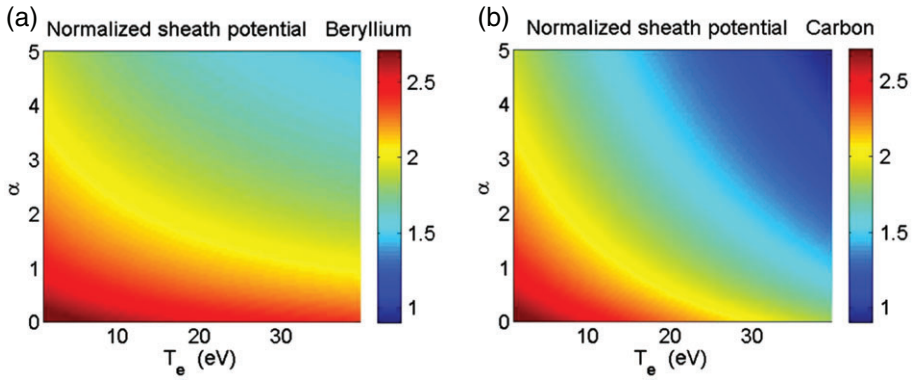

FIGURE 4 Normalized sheath potential (absolute value) as a function of electron and ion temperatures for (a) Be and (b) C walls.

Γ_{e2} increase with the increase in the electron temperature. According to Equation 13 or Equation 18, the increased Γ_{e2} causes φ_s to drop because of the current balance at the wall. For the same electron temperature, the potential drop across the sheath for the Mo wall is the largest among four materials because its δ_{eff} is the largest in the given ranges of the electron temperature $2\,\text{eV} < T_e < 40\,\text{eV}$, as shown in Figure 2b. The effect of the ion temperature on the sheath potential is shown in Figure 3b. When the ion temperature is increased, the increase of the ion current causes an increase in the electron current to keep the current balance at the wall. As a result, the potential drop across the sheath decreases with the increase in the ion temperature. Figure 4 displays comprehensively the variation of the normalized sheath potential with electron and ion temperatures for Be and C walls. In the given ranges of the electron temperature and α, the normalized sheath potential is a decreasing function of the ion and electron temperatures. It must be pointed out that Figure 4 only shows the variation of the normalized sheath potential as a function of ion and electron temperatures. Actually, the sheath potential always decreases with the increase in the electron temperature for a given α according to $\varphi = \frac{e_0\phi}{k_B T_e}$. From Figures 3 and 4, it is seen that the sheath potential has influence on the sheath energy transmission coefficient and impurity production when the electron and ion temperatures are changed.

Next we discuss the sheath energy transmission coefficient of the plasma sheath in the presence of SEE for a wide range of ion temperatures. The heat flow through the sheath arriving at the wall surface includes the contributions from the ion thermal energy, the electron thermal energy, and the energy derived by the ions due to their acceleration in the sheath potential. γ can be calculated as follows[23]:

$$\gamma = 2\alpha + \frac{2}{1-\delta_{eff}} - \varphi_s. \tag{20}$$

Results of γ are given in Figures 5 and 6 for different wall materials. We can see that γ depends strongly on the electron and ion temperatures. γ increases as the electron temperature increases. This is due to the fact that the number of electrons that reach the surface increases rapidly as δ_{eff} increases, although the ions are accelerated to a lesser extent. For the same electron temperature, γ is largest in the case of Mo wall because of the large δ_{eff}. The dependence of γ on the electron temperature indicates that the contributions of the electron thermal energy to γ is more important than the contribution of the energy derived by the ions due to acceleration in the sheath potential. For a certain value of electron temperature, γ increases as the ion temperature is increased, indicating that the increase of the ion thermal energy is larger than the decrease of the energy derived by ions due to acceleration in the sheath potential since the sheath potential decreases (as shown in Figure 3b). To explore the effect of SEE on γ in more detail, we show the dependence of γ on both the electron and ion temperatures for Be and C walls in Figure 6.

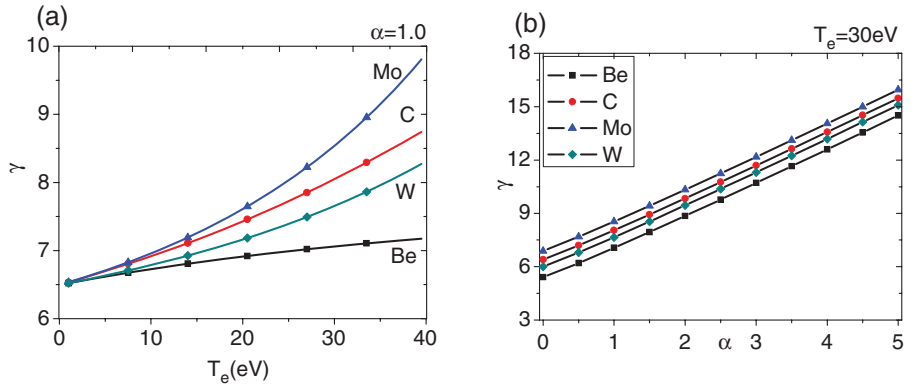

FIGURE 5 Sheath heat transmission coefficient for Be, C, Mo, and W walls as a function of electron temperature with (a) $\alpha = 1.0$ and (b) with $T_e = 30$ eV.

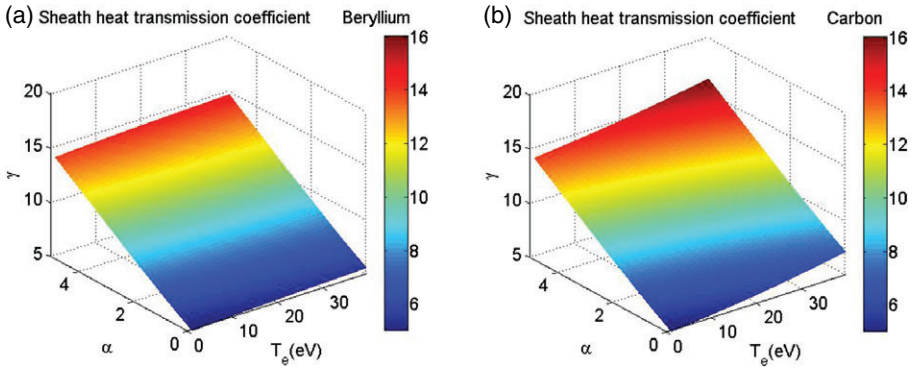

FIGURE 6 Sheath heat transmission coefficient as a function of electron and ion temperatures in two cases of (a) Be and (b) C as wall materials.

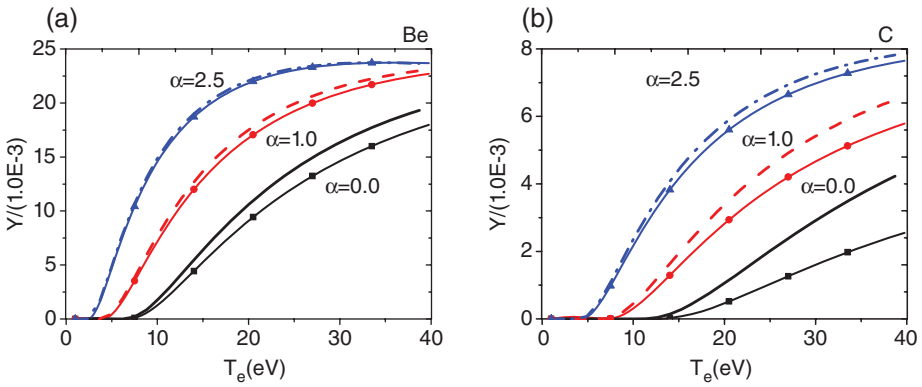

FIGURE 7 Sputtering yields as a function of electron temperature for Be and C walls in three cases of α ($\alpha = 0.0$ line with squares—with SEE, line—without SEE; $\alpha = 1.0$ line with circles—with SEE, dash—without SEE; $\alpha = 2.5$ line with triangle—with SEE, dash with dot—without SEE).

Usually, the heat flow through the sheath has influence on the sputtering yields, including physical and chemical sputtering. Here we discuss only physical sputtering. The Bohdansky formula, which is an empirical formula used widely to calculate the sputtering yield, can be written at normal incidence[31] as,

$$Y(E_i) = QS_n(E_i)\left(1 - \frac{E_{th}}{E_i}\right)^2 \left[1 - \left(\frac{E_{th}}{E_i}\right)^{2/3}\right], \tag{21}$$

where the parameter Q and the threshold energy E_{th} are used to fit the available data.[27] S_n for the Kr–C potential is given by,

$$S_n^{Krc}(E_i) = \frac{0.5\ln(1 + 1.2288E_i/E_{TF})}{E_i/E_{TF} + 0.1728\sqrt{E_i/E_{TF}} + 0.008(E_i/E_{TF})^{0.1504}}, \tag{22}$$

with a fixed parameter for each ion–target atom combination E_{TF}.[24] E_i is the energy of the ion arriving at the wall material, and it can be calculated from the contributions of the ion's thermal energy, kinetic energy before entering the sheath, and energy due to acceleration in the sheath:

$$E_i = 2k_BT_i + \frac{1}{2}m_iv_{iS}^2 - \varphi_sk_BT_e. \tag{23}$$

Here, Y for Mo and W wall materials are not discussed because of their small Q and high E_{th}.[27] Y for Be and C walls are shown in Figure 7 in two cases, namely with and without SEE. We can see that Y becomes small when SEE is taken into account. For small α, sputtering yield has a pronounced difference in the two cases with and without SEE. Especially for C wall, when SEE

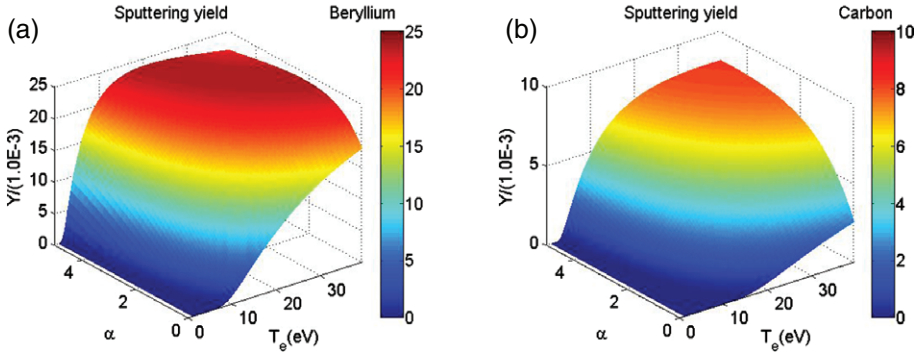

FIGURE 8 Sputtering yield as a function of electron and ion temperatures in two cases of (a) Be and (b) C walls.

is taken into account, sputtering yield is reduced obviously due to the effect of the large δ_{eff} on the contribution of the energy derived by acceleration in the sheath, compared to the case without SEE. The difference of Y decreases as the ion temperature is increased. The reason is that the ion's thermal energy and kinetic energy before entering the sheath dominate gradually the total energy arriving at the wall, while the energy derived by acceleration in the sheath becomes small. Since the material component lifetime and plasma contamination by the eroded surface atoms are the key issues for material choice in tokamak devices, Y as a function of the ion and electron temperatures are shown in Figure 8 for Be and C as wall materials when SEE is present.

4 | SUMMARY

In this paper, we presented numerical calculations of the energy transmission coefficient and sputtering yields of impurities over a wide range of ion temperatures when heat flows through the sheath in front of the negative walls emitting secondary electrons in contact with hydrogen plasmas. Based on an empirical estimation of the SEE for various materials, such as Be, C, Mo, and W, the effective SEE coefficient was calculated by integrating over the Maxwellian electron velocity distribution. Then the SEE yields were used to calculate the sheath potential by using a one-dimensional fluid model. It was found that both the electron and ion temperatures affect the sheath potential. Since the effective SEE coefficient is determined by the electron temperature, the sheath potential depends strongly on the wall materials due to the differences of the effective SEE coefficient. With increase in the ion temperature, the sheath potential decreases. The variation of sheath potential has influence on the sheath energy transmission and impurity sputtering yields. The energy transmission coefficient always varies with the wall material due to the effect of SEE, and it increases as the ion temperature increases. When comparing with and without SEE, in the former case the sputtering yield shows a significant decrease for small ion temperatures due to the large difference of the contribution of the energy derived by acceleration in the sheath and the energy of ions arriving at the surface. The difference decreases as the ion temperature increases, indicating that the contribution of the energy derived by acceleration in the sheath decreases while both the ions' thermal energy and kinetic energy before entering the sheath increase.

Finally, it must be pointed out that the electron temperature is in the range $2\text{eV} < T_e < 40\,\text{eV}$ in our model. For some wall materials such as Mo and W, if the electron temperature is high, the SCL state may be broken because of the occurrence of the very large influx of emitted electrons in the sheath. Under this condition, the variation of the potential in the sheath is not monotonic, and the effect of SEE on the sheath structure in this case will be studied in future.

ACKNOWLEDGMENTS

This work was supported by National Natural Science Foundation of China (nos.11475223 and 11105176), the National Magnetic Confinement Fusion Science Programme of China (no. 2015GB101003), and the programme of Fusion Reactor Physics and Digital Tokamak with the CAS "One-Three-Five" Strategic Planning.

REFERENCES

[1] G. D. Hobbs, J. A. Wesson, *Plasma Phys.* **1967**, *9*, 85.
[2] J. Seon, E. Lee, *Plasma Sci. Tech.* **2013**, *15*, 1093.
[3] S. Takamura, M. Y. Ye, T. Kuwabara, N. Ohno, *Phys. Plasma.* **1998**, *5*, 2151.
[4] T. Gyergyek, J. Kovacic, M. Cercek, *Contrib. Plasma Phys.* **2010**, *50*, 121.
[5] S. Takamura, N. Ohno, M. Y. Ye, T. Kuwabara, *Contrib. Plasma Phys.* **2004**, *44*, 126.
[6] X. Zhao, N. Xiang, J. Ou, D. Li, B. Lin, *Chin. Phys. B* **2016**, *25*, 025202.
[7] J. Ou, B. Lin, X. Zhao, Y. Yang, *Plasma Phys. Control. Fusion* **2016**, *58*, 075004.
[8] R. N. Franklin, W. E. Han, *Plasma Phys. Control. Fusion* **1988**, *30*, 771.
[9] J. P. Sheehan, I. D. Kaganovich, H. Wang, D. Sydorenko, Y. Raitses, N. Hershkowitz, *Phys. Plasma.* **2014**, *21*, 063502.
[10] J. M. Pedgley, G. M. McCracken, *Plasma Phys. Control. Fusion* **1993**, *35*, 397.

[11] I. V. Tsvetkov, T. Tanabe, *J. Nucl. Materials* **1999**, *266–269*, 714.
[12] R. Chodura, *Phys. Fluids* **1982**, *25*, 1628.
[13] J. Lui, F. Wang, J. Sun, *Phys. Plasma.* **2011**, *18*, 013506.
[14] M. Khoramabadi, H. Ghomi, P. K. Shukla, *J. Appl. Phys.* **2011**, *109*, 073307.
[15] J. Ou, J. Yang, *Phys. Plasma.* **2012**, *19*, 113504.
[16] K.-U. Riemann, *Phys. Plasma.* **1997**, *4*(11), 4158.
[17] T. Gyergyek, J. Kovacic, *Phys. Plasma.* **2015**, *22*, 093511.
[18] H. Y. Huo, G. F. Matthews, S. J. Davies, S. K. Erents, L. D. Horton, R. D. Monk, P. C. Stangeby, *Contrib. Plasma Phys.* **1996**, *46*, S81.
[19] M. Kocan, J. P. Gunn, J.-Y. Pascal, G. Bonhomme, C. Fenzi, E. Gauthier, J.-L. Segui, *Plasma Phys. Control. Fusion* **2008**, *50*, 125009.
[20] M. Kocan, J. P. Gunn, S. Carpentier-Chouchana, A. Herrmann, A. Kirk, M. Komm, H. W. Muller, J.-Y. Pascal, R. A. Pitts, V. Rohde, P. Tamain, *J. Nucl. Mater.* **2011**, *415*, S1133.
[21] D. Brunner, B. LaBombard, R. M. Churchill, J. Hughes, B. Lipschultz, R. Ochoukov, T. D. Rognlien, C. Theiler, J. Walk, M. V. Umansky, D. Whyte, *Plasma Phys. Control. Fusion* **2013**, *55*, 095010.
[22] P. C. Stangeby, *Phys. Fluid* **1984**, *27*, 682.
[23] P. C. Stangeby, in *Physics of Plasma-Wall Interaction in Controlled Fusion* (Eds: D. E. Post, R. Behrisch), Plenum, New York **1986**, p. 41.
[24] W. Eckstein, C. Garcıa-Rosales, J. Roth, W. Ottenberger, Sputtering Data, Report IPP 9/82, Max Planck Institut fur Plasmaphysik, Garching, **1993**. http://hdl.handle.net/11858/00-001M-0000-0027-6324-6
[25] D. Bohm, in *The Characteristics of Electrical Discharges in Magnetic Field* (Eds: A. Guthry, P. K. Wakerling), McGraw-Hill, New York **1949**.
[26] K. U. Riemann, *J. Tech. Phys.* **2000**, *41*, 89.
[27] P. C. Stangeby, *The Plasma Boundary of Magnetic Fusion Devices*, IOP Publishing, Bristol **2000**.
[28] T. Tawaraya, A. Tsushima, S. Yoshimura, *Jpn. J. Appl. Phys.* **2012**, *51*, 096101.
[29] E. J. Sternglass, *Theory of Secondary Electron Emission, Scientific Paper 1772*, The Westinghouse Research Laboratory, Pittsburgh, PA **1954**.
[30] W. Li, J. Ma, J. Li, Y. Zheng, M. Tan, *Phys. Plasma.* **2012**, *19*, 030704.
[31] J. Bohdansky, *Nucl. Instrum. Methods B* **1984**, *2*, 587.

How to cite this article: Ou J, Zhao X. Heat flow through a plasma sheath in the presence of secondary electron emission from plasma-wall interaction. *Contrib. Plasma Phys.* 2017;57:50–57. https://doi.org/10.1002/ctpp.201600043